

Prediction of Critical Bed Load Transport Zones with the Presence of Protruding Stable Clast in a Mountain River Reach

Shanker Kumar Sinnakaudan, Mohd Rizal Shukor, and Mohd Sofiyan Sulaiman

Abstract— A field study was conducted to examine the influence of naturally formed protruding stable clast on the bed load transport mechanism. ArcGIS Spatial Analyst was used to graphically evaluate the influence of bed shear stress on bed load transport zones. High magnitude of bed shear stress that corresponds with the prevalent bed load transport activities was found to be concentrated on lower bed elevation zone. On the other hand, sheltering effect existed on the zone behind the protruding cobble thus result weak or zero bed load transport actions. The derived critical bed load transport zones then were further confirmed by the zonation of sweeps and ejections event from turbulent bursting cycle. The most transported bed load was found to be coincided with high magnitude of sweeps and ejections events. Thus, the critical and suitable bed load sampling points can be correctly identified for future applications based on the methodology demonstrated.

Keywords— Bed Load, Mountain Rivers, Shear Stress, Stable Clast.

I. INTRODUCTION

PROTRUDING stable clast that having low relative submergence was among the vital morphological features found on the Mountain Rivers in Malaysia. The availability of these protruding elements alters the turbulent characteristics of flow thus make bed load transport varies spatially [1]. Typical physical bed load transport measurements require the deployment of device (Helley-Smith or bed load trap) at either equal-space distribution [2] or uneven spacing [3] across the stream. The measurement can be underestimated or overestimated as compared to the actual rate of transport if the bed load traps were sampled at the wrong locations due to unidentified location of active bed load transport zones. So far, there is no attempts have been made to identify potential bed load transport

location before bed load sampling is carried out on site. Thus, determination of potential bed load transport location with aid of desecrate spatial analysis tools is imperative in having accurate prediction of streambed erosion and sedimentation. Thus, the aims of the present study are to derive critical bed load transport location/s by coupling the turbulence properties with the bed load transport data.

II. STUDY AREA

The field study was conducted at Rasil River which situated within Pasir Akar drainage basin of Hulu Besut, Terengganu State, Malaysia (Fig. 1). Rasil River is a sand-gravel bed river that comprised of sand to small boulder type of bed material. The existence of protruding boulders which having low relative submergence is prominent morphological feature at the study reach. The view of protruding element on study reaches is clearly shown in the Fig. 2. Protruding clast in this study is define as single protruding boulder (intermediate axis size ranging from 45cm-84cm) which having low relative submergence that immobile during base flow condition. Rasil River is one of the many tributaries that drain into Besut River which to be found about 48 meters above the mean sea level and the final discharge of the flow is at South China Sea. Besut River was among the problematic river in Malaysia that reported major flood to the surrounding area nearly every year. Recent Studies confirmed that excessive development particularly on mountain river basin in Malaysia might result this phenomena [4].

Shanker Kumar Sinnakaudan is Head of Water Resources Engineering and Management Research Centre (WAREM) and Associate Professor at Faculty of Civil Engineering, Universiti Teknologi MARA Pulau Pinang, 13500 Permatang Pauh, Penang, Malaysia (Corresponding Author's Phone: +6045402438; e-mail: drsshah@yahoo.com).

Mohd Rizal Shukor is a Graduate Student, Dept. of Civil Engineering, Universiti Teknologi MARA, 13500 Permatang Pauh, Penang, Malaysia (e-mail: mohdrizal50@yahoo.com).

Mohd Sofiyan Sulaiman is a Ph.D student, Dept. of Civil Engineering, Universiti Teknologi MARA, 13500 Permatang Pauh, Penang, Malaysia (e-mail: mohd.sofiyan@yahoo.com)

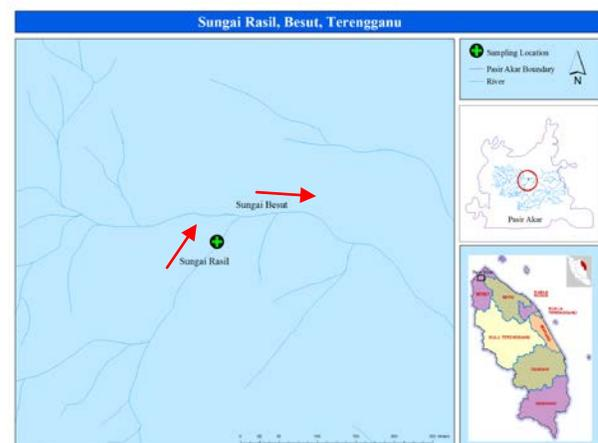


Fig. 1 Study Area



Fig. 2 Sediment Transport around the Protruding Clast

III. DATA COLLECTION

The field data collection was conducted during February to March of year 2011. The entire field measurement was conducted on bright and sunny day with no raining is recorded. The flow condition of study reaches is recorded at a depth approximately varies from 0.27m to 0.33m. The average flow velocity recorded is 0.27 m/s to 0.365 m/s which are suitable for wading technique to be employed. It is observed that the velocity and flow depth is stable during the sampling period. Besides that, the stream discharge is between $1.197\text{m}^3/\text{s}$ to $1.795\text{m}^3/\text{s}$. The turbulent flow regime account for all study reaches with subcritical flow ($Fr < 1$) indicating slow and tranquil flow. The energy gradient measured for downstream is 0.6% and for upstream 0.1%. The Manning's roughness coefficient obtained here varies from 0.024 to 0.026 which in accordance with the value provided by [5] which confirms that roughness value for sand-gravel bed river should lies between 0.012 until 0.035. The study was conducted at a straight reach where the presence of stable clast prominent within the reach (Fig. 3).



Fig. 3 Study Reach

Pre-fixed spatial coordinate reference system is used to morphologically describe the river bed topography of study area. A 6m x 6m (x-axis versus y-axis) grid was prepared for selected reach where by the selected protruding clast is within the bounding grid. Auto-level was set at a fixed position and the bed elevation was measured at every 0.2m increment at each axis. These spot heights were recorded as z-axis value and the similar procedure continued until entire study grids are successfully covered. Fig. 4 illustrated the view of study area with spatial coordinate reference system. By having three dimensional coordinate (x, y and z), surface bed topography of study reaches then generated by using ArcGIS Spatial and 3D Analyst.



Fig. 4 Spatial Coordinate Measurement

Turbulence properties in this study are represented by bed shear stress (τ_b) and turbulent bursting events. Both parameters are derived from turbulence flow velocity data. In recent study, Nortek ADV Vector was deployed to collect turbulence velocity data. ADV is a point velocity measurement device that can measure 3 dimensional velocities at high frequency. The velocity was measured in point profile measurement. Velocity profile measurement is essential in determination of bed shear stress [6]. There are various methods available in bed shear stress estimation and different method could give different results. Recent study adopts four different methods to estimate bed shear stress as illustrated in Table I.

TABLE I
METHODS TO ESTIMATE BED SHEAR STRESS

Approach	Equation	Researcher
1. Log-law	$\frac{\bar{u}}{u_*} = \frac{1}{k} \ln \left(\frac{z + z_o}{k_s} \right) + B$ $u_* = \sqrt{(\tau_o / \rho)}$	[6], [7]
2. Reynolds Stress	$\tau_o = -\rho \langle u' w' \rangle$ (extrapolate to bed) (used near bed value)	[1], [6], [7], [8], [9], [10], [11]
3. Turbulent Kinetic Energy (TKE)	$\tau_o = C_1 [0.5\rho(u'^2 + v'^2 + w'^2)]$	[6], [7], [8], [9]

where \bar{u} is mean velocity, u_* is shear velocity, z is height above the bed, z_o is the characteristic roughness length, k is von Karman's constant (taken to be 0.4), k_s is roughness height, B is roughness constant (taken 8.5 for fully rough flow), C_1 is proportionally constant (taking as 0.19) while u' , v' and w' represents fluctuations of velocity component for streamwise, spanwise and vertical respectively.

Portable Helley-Smith sampler was used to collect the bed load samples. The bed load measurement was done at the same spot as turbulence velocity measurement. 12 sampling points were selected around the stable to represent spatial distribution of bed load and turbulent flow (Fig. 5).



Fig. 5 Spatial Bed Load and Turbulence Flow Measurement

The bed load transport rate is very much depending on its sampling duration [3]. Generally, five to ten minutes of sampling duration is adopted depending on flow intensity of study reach [2]. Since the recent study only restricted to low flow regime, one hour of sampling period was selected as to diminish the temporal variation of bed load transport rate. The selection of one hour sampling duration is in accordance with finding from [13] that one hour sampling duration can provide

sufficient time to move large particle size near the threshold of motion. Equation (1) and (2) are the typical equation used to calculate bed load transport rate for study reaches as proposed by [2].

$$G_b = \frac{W_i}{(T * h_s) * b} \tag{1}$$

$$T_b = \sum_{n=1}^8 G_b \tag{2}$$

Where G_b is bed load rate (kg/s), W_i is weight of sample, T is sampling duration, h_s is width of sampler entrance, b is ratio of stream width to the number of sampling sections and T_b = rate of bed load transport for a given cross section (kg/s). The bed load samples collected in the sampler will be dried, weighted and sieved to obtain the time-averaged bed load transport rate for the duration of measurements and the composition of the bed load.

IV. METHODOLOGY

Geographic Information System (GIS) was used as a tool to analyze and generate potential bed load transport zones for study reaches. Potential bed load transport zones were derived based on graphical correlation between bed shear stress and measured bed load transport data. The correlation was yield based on overlay operation using ArcGIS Spatial Analysis 9.3 on various spatial parameters. In this study, spatial analysis was done in three different stages.

At the first stage, the study reach geometry data was imported into ArcGIS as point file with site specific coordinate system as determined earlier during the field survey. The Digital Elevation Model (DEM) for the study reach was created using 'Spline' method with cell size of 0.01 meters. A contour map was generated from the DEM with contour interval of 1 meter.

The emergence surface of the stable class are considered to be a hydraulic barrier and assumed no sediment transport or flow occurred above the water surface elevation. Thus, the stable class was digitized as a polygon feature based on 3D view of the study reach which was created in ArcScene. The DEM of the study reach was further refined by creating a Triangular Irregular Network (TIN) model which allows the stable class polygon file to be used as hard breaklines during the surface creation process. The hard break line indicates the inactive zone of flow and sediment transport in the study reach and incorporated when bed shear stress DEM model created in the later stage. The typical steps followed are shown in Fig. 6.

Subsequently, bed shear stress and bed load contours were derived from bed shear stress and bed load DEMs. The DEMs created by using Spline with Barrier Interpolation method whereby the digitized stable clasts are used as a hydraulic barrier. The overlay analysis was later used to find out the correlation between three spatial parameters namely bed topography, bed shear stress and bed load rate. The correlation results was used as a guide to derive critical bed load transport zones with two main criteria's; (1) consistency of plot from

various methods of bed shear stress estimation toward bed topography; (2) active bed load transport zones based on sweeps and ejection phenomenon. Predicted zones then were further verified by actual measured bed load transport rate.

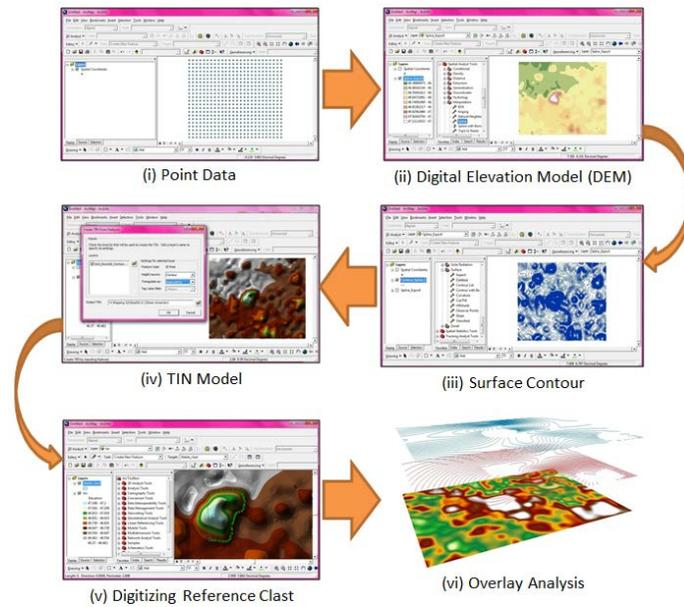


Fig. 6 Mapping Methodology with ArcGIS Desktop 9.3

V. RESULT AND DISCUSSION

A. Bed Shear Stress Spatial Analysis

Analysis of bed shear stress was done based on responds of different bed shear stress estimators toward the stable clast. The patterns of bed shear stress estimated were evaluated against bed elevation TIN. Fig. 7(a-d) shows the pattern of plot for bed shear stress (contour lines) towards bed elevation. It was evident that bed shear stress estimated by Log-law approach dominating on the higher bed elevation zone which has shallow water depth. The maximum bed shear stress recorded is 6.8 N/m² which was located on the stoss zone, 1 meter in front of the reference clast as shown in Fig. 7a. However, higher bed shear stress value (25 N/m²) was found on the lower elevation zone, to be exact at the side zone which approximately 1 meter beside the reference clast for Reynolds extrapolated method (Fig. 7b). Much similar pattern also recorded for TKE and Reynolds single point methods. TKE method gives the highest bed shear stress estimation compared to other methods. The maximum value (48 N/m²) was recorded at the same spot as Reynolds extrapolated method (Fig. 7c). It is 47% greater than Reynolds extrapolated estimation. Fig. 7d portrays the maximum bed shear stress estimation obtained from Reynolds single-point method that concentrated on the same location as Reynolds extrapolated and TKE method. All shear stress methods except for the Log-law method reported the maximum value at the lower bed elevation zone. Lower bed elevation reflects greater water depth thus indicating that bed shear stress more dominant on the deeper water.

It is interesting to note that the lee zone was described as the location of low bed shear stress production by all the four methods used. Again TKE method gives the highest estimation of bed shear stress at the value of 4 N/m² for this zone and the lowest estimation comes from Log-law method at 1.6 N/m². The least bed shear stress estimation zone might due to obstruction provided by the protruding clast. The protruding clast decelerates the velocity behind the clast thus making shear stress production decreased. This low value was continued until downstream zone from the reference clast. However, upstream zone reported fair value for bed shear stress ranging from 1.6–4.8 N/m² for Log-law method, 3–16 N/m² for Reynolds extrapolated method, 3–32 N/m² for TKE method and 0–10.5 N/m² for Reynolds single point method. Once again TKE method gives the highest estimation compared to other methods. So far, the side zone was considered as the critical location for bed shear stress production for all methods.

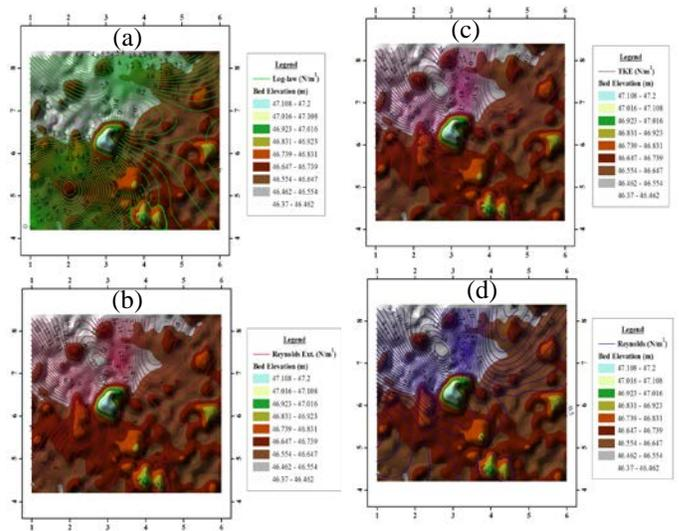


Fig. 7 Bed Shear Stress Spatial Analysis

Log-law method estimates maximum value on left side from the reference clast while another three methods recorded maximum value on the right side zone of the reference clast. Based on these results, it can be concluded that the location of active bed shear stress locations may located on the side zone, 1 meter from the reference clast. Due to existence partial submergence protruding element, the flowing water deflected towards side zone thus creating scour zone. At the scour zone, vortex shedding pattern clearly seen on both side zones (left and right side) from the reference clast.

B. Dominant Turbulent Event in Bed Shear Stress Production

Quadrant analysis was performed to describe the general motion of turbulent fluid in vicinity of protruding clast. Four turbulent bursting events were examined by high magnitude of turbulent bursting event (hole size, H=2.5). Hole size, H=2.5 was selected in accordance with previous studies [14], [8]. Sweeps event was the strong movement of fluid towards bed

that typically related with bed load motion while ejections event is slow fluid movement away from the bed which related with suspended load motion. These two events had been reported dominating shear stress production by many researchers [11], [14], [10]. Fig. 8a shows that maximum bed shear stress from Log-law method was found on the sweeps region (blue colour) which agrees with [11], [14], [10].

However, Log-law method also found to be estimating least bed shear stress on sweeps region. This may indicate that bed shear stress estimated from log-law method do not have any consistent spatial pattern with turbulent bursting cycle. For Reynolds extrapolated method, maximum bed shear stress estimation was found on ejections region (light yellow colour) as shown in Fig. 8b. Comparable bed shear stress value also obtained at outward-interactions region (Q1) which agrees with laboratory analysis results reported by [15]. On the other hand, the lowest bed shear stress estimation was recorded on transition region between inward-interaction region (Q3) and ejections region. The identical pattern also found for TKE method (Fig. 8c) and Reynolds single-point method (Fig. 8d). The only different was that the value obtained from TKE method comparatively higher for all regions rather than Reynolds extrapolated method while the pattern of the plot was still looks alike.

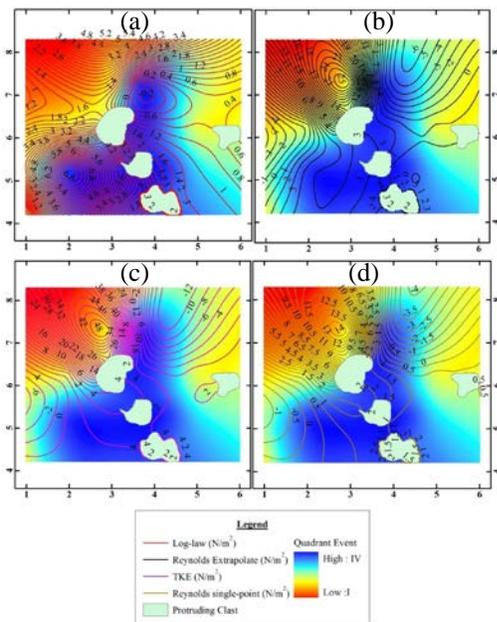


Fig. 8 Bed Shear Stress Spatial Analysis

C. Conformity of Turbulent Characteristics with Bed Load Motion

Accuracy of near-bed shear stress to predict bed load transport zone was assessed via overlay analysis. Fig. 9(a-d) depicts the results obtained from different methods of bed shear stress estimation over measured bed load transport DEM where the dark brown colors indicate active bed load transport zone while light pink color represent the least bed load transport zone. Graphically, it can be said that Log-law method

do not show a good correlation with measured bed load transport rate as shown in Fig. 9a. Higher bed shear stress was found on weak bed load transport zone. However, Reynolds extrapolated; TKE and Reynolds single-point gave clear evidence that the most transported bed load zone was associated with higher bed shear stress (Fig. 9b-d). As mentioned earlier, TKE method gives the highest bed shear stress estimation followed by Reynolds extrapolate method and Reynolds single-point method. However, uncertainties in beam error associated with lateral velocity component mentioned by [6] might introduce bias into TKE estimation thus causing high bed shear stress value. By considering this condition, Reynolds extrapolate method should be used to estimate bed shear stress when turbulent velocity profile measurement is available.

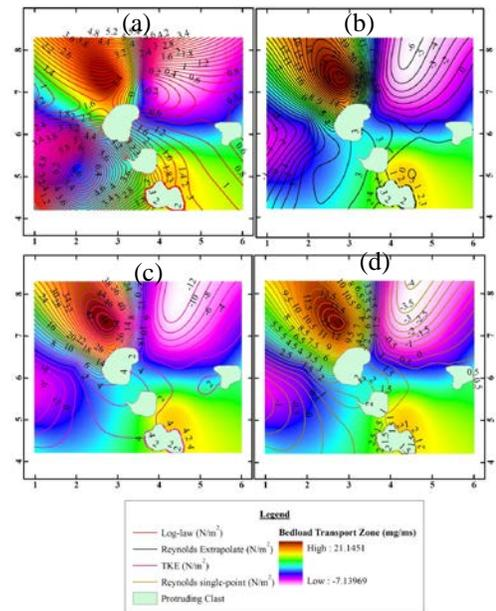


Fig. 9 Bed Shear Stress versus Bed Load Transport Rate

D. Verification of Critical Bed Load Transport Zones

The reliability of derived critical bed load transport zones were further verified by conducting bed load transport measurement on identified critical bed load transport zones on 25th June 2012. Critical bed load transport zones here were assessed via two conditions; 1) measured bed load by individual point sampling; 2) measured bed load transport by reach-average value. In order to reduce bias to the analysis due to temporal variation of measurement, the hydraulic condition and geometry shape of river was rechecked to re-confirm that the bed is stable and no significant changes occurred to the bed morphology as compared to the previous data collection visits. Besides that, no bank full discharges which may alter the bed morphology observed between the two sampling period. The flow velocity and flow depth measured were within the acceptable range of the present studies scope. Reach-average value of bed load transport was measured at the computed by using equation (1) and (2). Bed load sampling for the first visit was done at equal space along the transverse of the river. Five

sampling points measurement were selected to represent reach-average value of bed load for that transverse.

For the second visit, bed load point sampling locations were sorted based on the critical bed load transport zones map. Three sampling points were distributed on the most transported bed load while another two points concentrated on the less transported zones. No bed load measurement was done on the zone behind the stable clast due to zero bed load transported zone predicted there. The contrast of bed load sampling point distribution between the first visit and the second visit is illustrated in Fig. 10.

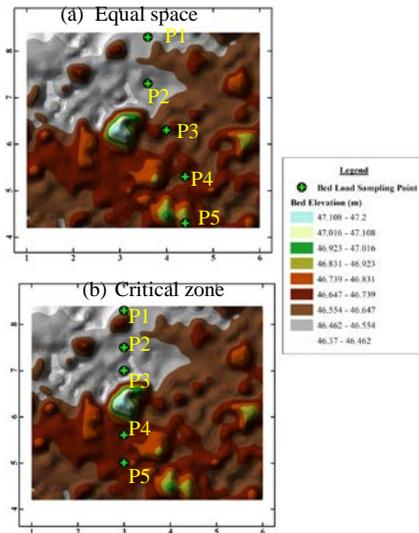


Fig. 10 Bed Load Sampling Point Distribution between two visits

It is interesting to be noted that all new sampling points located at the critical bed load transport zone showing an increment in the measured bed load as compared to the equal space sampling. It was found that, the highest measured bed load rate for the second visit concentrated on the identified critical zone. 72.47 mg/ms of bed load rate was recorded on P2 which is 276% greater than the highest bed load rate measured from the first visit (Fig. 11). Meanwhile, comparable higher bed load rate also was found on at the location beside the highest point for the second visit data set. Both points, P1 and P3 recorded 18.36 mg/ms and 36.17 mg/ms of bed load motion respectively. These two point located on the same zone as the highest measured bed load rate which on the lower bed elevation area. This result gives further evidence to support the findings that the lower bed elevation is the concentration zone for vigorous bed load transport activities. In the meantime, reach-average value of bed load transport was found significantly increased when the sampler is set up on the right location or at the critical bed load transport zones. Fig. 11 summarizes the result from reach-average value analysis. By deploying the bed load sampler at equal space along the transverse, 92.637 mg/s of bed load motion was trapped. However, by deploying the bed load samplers on the proposed location based on identified critical zones, significant increase in reach-average value of

bed load transport rate was recorded. The result proves that by putting the sampler on the right location increase the reach-average bed load transport measurement for almost 363% rather than equal space deployment method.

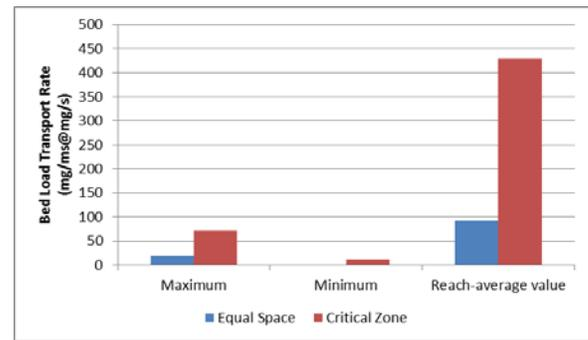


Fig. 11 Sampling Point Distribution between two visits

VI. CONCLUSION

Result from high magnitude of turbulent event ($H=2.5$) reveals that ejections event dominating region adjacent to protruding clast particularly at lower bed elevation regions. These findings are consistent with previous work done by [10] and [11] that ejection events dominating near bed region adjacent to protruding element. Sweeps event was reported controlling the region behind the clast and focusing at high bed elevation. While traveling downstream, inward-interaction event tends to be dominant. Apart from that, the association between near bed shear stress with turbulent bursting event clearly defined. The location of maximum bed shear stress was found to be governed by ejections event. This is proved by identical estimation by three different bed shear stress methods namely TKE, Reynolds extrapolate and Reynolds single-point method. However, sweeps event that mostly linked with bed load motion was found to be match with high bed shear stress from Log-law method at shallow water depth. Nevertheless, further justification is needed due to inconsistent estimation by Log-law method towards bed elevation and turbulent bursting event.

On the other hand, recorded weakest bed load transport zone was on lee zone. Lee zone here is characterized by high bed elevation and slow moving flow. Bed shear stress reported on this zone also slightly low. It is widely accepted that the particle (bed load) started to move when its critical shear stress value was exceeded. The critical shear stress value is very much depending on the relative particle size within a reach [16], [17]. Larger particles may have larger critical shear stress thus require larger bed shear stress to initiate the motion. In this study, protruding element acts as barrier that shielding smaller particle from being transported. As such, in order to transport the smaller particle behind the clast, the larger particle needs to be transported first. This indirectly may also require larger shear stress to transport the smaller particle behind that clast. The phenomenon give some limelight on why the zone behind the clast which associates with low bed shear stress was the least zone for bed load transport activities. Fi-

nally the critical location of bed load transport was derived based on the findings that the most transported zone for bed load coincides with high bed shear stress value. It was found that the partially submerged protruding clast dispersed the flow aside. With the aid of slow moving flow away from the bed (ejections event), some of the particles start rolling and sliding over the bed and concentrated on low bed elevation zone. Even though the ejections event was previously reported by many re-searchers that responsible for suspended load motions, however its contribution over bed load motion also cannot be denied.

ACKNOWLEDGMENT

We would like to thank the Ministry of Science, Technology and Innovation (MOSTI) for funding this research by awarding Sciencefund (04-01-01-SF0250) and through “Dana Kecemerlangan UiTM” grant (600-RMI/ST/DANA 5/3Dst). Many thanks also due to Water Resources Engineering and Management Research Centre (WAREM) and Faculty of Civil Engineering UiTM Penang for their support and encouragement to conduct this research successfully. Special gratitude to Dr. Kyle Strom from Department of Civil and Environmental Engineering, University of Houston, Texas for providing valuable comments and ideas throughout the research period.

REFERENCES

- [1] A. N. Papanicolaou, P. Diplas, C. L. Dancy, and M. Balakrishnan, “Surface roughness effects in near-bed turbulence: Implications to sediment entrainment”, *Journal of Engineering Mechanics*, 127(3), pp. 211-218, 2001.
[http://dx.doi.org/10.1061/\(ASCE\)0733-9399\(2001\)127:3\(211\)](http://dx.doi.org/10.1061/(ASCE)0733-9399(2001)127:3(211))
- [2] DID-Department of Irrigation, Drainage Malaysia, “River Sediment data Collection and Analysis Study (Final Report)”, Department of Irrigation and Drainage Malaysia, Kuala Lumpur, 2003.
- [3] K. Bunte, K. W. Swingle, and S. R. Abt, “Guidelines for using bedload traps in coarse-bedded mountain streams: Construction, installation, operation, and sample processing”, General Technical Report RMRS-GTR-191. Fort Collins, CO: U.S. Department of Agriculture, Forest Service, Rocky Mountain Research Station, 91, 2007.
- [4] S. K. Sinnakaudan, M. S. Sulaiman, S. H. Teoh, “Total bed material load equation for high gradient rivers”, *Journal of Hydro-environment Research*, Vol. 4, pp. 243-251, 2010.
<http://dx.doi.org/10.1016/j.jher.2010.04.018>
- [5] G. J. Jr. Arcment, and V. R. Schneider, “Guide for Selecting Manning’s Roughness Coefficients for Natural Channels and Flood Plains”, *USGS Water Supply Paper*, 2339, 1984.
- [6] P. M. Biron, C. Robson, M. F. Lapointe, and S. J. Gaskin, “Comparing different methods of bed shear stress estimates in simple and complex flow fields”, *Earth Surface Processes and Landforms*, 29, pp. 1403-1415, 2004.
<http://dx.doi.org/10.1002/esp.1111>
- [7] M. S. Sulaiman, S. K. Sinnakaudan, and M. R. Shukor, “Near Bed Turbulence Measurement with Acoustic Doppler Velocimeter (ADV)”, *KSCE Journal of Civil Engineering*, 17(6), pp. 1515 – 1528, 2013.
<http://dx.doi.org/10.1007/s12205-013-0084-8>
- [8] R. W. J. Lacey and A. G. Roy, “The spatial characterization of turbulence around large roughness elements in a gravel-bed river”, *Geomorphology*, 102, pp. 542-553, 2008.
<http://dx.doi.org/10.1016/j.geomorph.2008.05.045>
- [9] A. Robert, “River Process: An Introduction to Fluvial Dynamics. London: Hodder Education, 2003.
- [10] T. Buffin-Belanger, and A. G. Roy, “Effects of a pebble cluster on the turbulent structure of a depth-limited flow in a gravel-bed river”, *Geomorphology*, 25, pp. 249-267, 1998.
[http://dx.doi.org/10.1016/S0169-555X\(98\)00062-2](http://dx.doi.org/10.1016/S0169-555X(98)00062-2)
- [11] A. Robert, A. G. Roy, and B. D. Serres, “Turbulence at a roughness transition in a depth limited flow over a gravel bed”, *Geomorphology*, 16, pp. 175-187, 1996.
[http://dx.doi.org/10.1016/0169-555X\(95\)00143-S](http://dx.doi.org/10.1016/0169-555X(95)00143-S)
- [12] J. M. Gaudet, A. G. Roy, and J. L. Best, “Effect of orientation and size of Helley-Smith sampler on its efficiency”, *Journal of Hydraulic Engineering*, 120(6), pp. 758-766, 1994.
[http://dx.doi.org/10.1061/\(ASCE\)0733-9429\(1994\)120:6\(758\)](http://dx.doi.org/10.1061/(ASCE)0733-9429(1994)120:6(758))
- [13] K. Bunte and S. R. Abt., “Sampler size and sampling time affect bed load transport rates and particle sizes measured with bed load traps in gravel-bed streams”, *Erosion and Sediment Transport Measurement in Rivers: Technological and Methodological Advances*, IAHS Publ. No. 283, pp. 126-133, 2003.
- [14] K. B. Strom and A. N. Papanicolaou, “ADV measurements around a cluster microform in a shallow mountain stream”, *Journal of Hydraulic Engineering*, 133(12), pp. 1379-1389, 2007.
[http://dx.doi.org/10.1061/\(ASCE\)0733-9429\(2007\)133:12\(1379\)](http://dx.doi.org/10.1061/(ASCE)0733-9429(2007)133:12(1379))
- [15] J. M. Nelson, R. L. Shreve and S. R. McLean, “Role of near-bed turbulence structure in bed load transport and bed form mechanics”, *Water Resources Research*, 31(8), pp. 2071-2086, 1995.
<http://dx.doi.org/10.1029/95WR00976>
- [16] L. K. Sarker and M. M. Hossain, “Shear stress for initiation of motion of median sized sediment of non-uniform sediment mixtures”, *Journal of Civil Engineering*, 34(2), pp. 103-114, 2006.
- [17] A. B. Shvidchenko, G. Pender and T. B. Hoey, “Critical shear stress for incipient motion of sand/gravel streambeds. *Water Resources Research*, 37(8), pp. 2273-2283, 2001.
<http://dx.doi.org/10.1029/2000WR000036>